J|A|C|S
ARTICLES
Published on Web 04/07/2006

Molecular Motion of Tethered Molecules in Bulk and Surface-Functionalized Materials: A Comparative Study of Confinement

Jessica L. Defreese,[†,§] Son-Jong Hwang,[‡] A. Nicholas G. Parra-Vasquez,[†,||] and Alexander Katz*[,†]

Contribution from the Department of Chemical Engineering, University of California, Berkeley, Berkeley, California 94720-1462, and the Division of Chemistry and Chemical Engineering, California Institute of Technology, Pasadena, California 91125

Received August 31, 2005; E-mail: katz@cchem.berkeley.edu

Abstract: Achieving high degrees of molecular confinement in materials is a difficult synthetic challenge that is critical for understanding supramolecular chemistry on solid surfaces and control of host−guest complexation for selective adsorption and heterogeneous catalysis. In this Article, using ^{2}H MAS NMR spectroscopy of tethered carbamates as a molecular probe, we systematically investigate the degree of steric confinement within three types of materials: two-dimensional silica surface, bulk amorphous microporous silica, and bulk amorphous mesoporous silica. The resulting NMR spectra are described with a simple two-site hopping model for motion and prove that the bulk silica network severely limits the molecular mobility of the immobilized carbamate at room temperature to the same degree as surface-functionalized materials at low-temperatures (∼210 K). Raising the temperature of the bulk materials to 413 K still demonstrates the effect of confinement, as manifested in significantly longer characteristic times for the immobilized carbamate relative to surface-functionalized materials at room temperature. The environment surrounding the carbonyl functionality of the immobilized carbamate is investigated using FT-IR spectroscopy, which shows the carbonyl stretching band to be equally shifted for all materials to lower wavenumbers relative to its noninteracting value in carbon tetrachloride solvent. These results suggest that electrostatic interactions between the carbonyl of the immobilized carbamate and silica surface may play an important role in confining the immobilized carbamate and nucleating the formation of a pore wall close to the immobilized carbamate during bulk materials synthesis.

Introduction

Molecular confinement is a hallmark of biological catalysts and molecular receptors.[1−5] The degree of confinement in protein active sites facilitates stereoselective molecular recognition and catalysis.[4,6,7] The beneficial effect of confinement on stereoselective transformations has also been demonstrated in synthetic catalysts,[8−14] photocatalysts,[15] and binding sites.[16−19] Confinement facilitates multiple points of contact between a guest molecule and the chiral host active site,[4] a general condition that is desired for stereoselective control of chemical reactivity.[16] However, the high degree of molecular confinement that is typical of biological active sites has heretofore been difficult to reproduce in synthetic systems.[5,20]

The molecular motion of an entity occluded within a host active site can be used as a local probe of environment that correlates inversely with degree of molecular confinement. The motion of occluded molecules within bulk crystalline materials

[†] University of California, Berkeley.
[‡] California Institute of Technology.
[§] Current address: Process Research and Development, Bristol-Myers Squibb Co., New Brunswick, NJ 08903-0191.
[||] Current address: Chemical and Biomolecular Engineering Department, Rice University, Houston, TX 77005.

(1) Richards, F. M. *Annu. Rev. Biophys. Bioeng.* **1977**, *6*, 151−176.
(2) Klapper, M. H. *Prog. Bioorg. Chem.* **1973**, *2*, 55−133.
(3) Klapper, M. H. *Biochim. Biophys. Acta* **1971**, *229*, 557−566.
(4) Sundaresan, V.; Abrol, R. *Protein Sci.* **2002**, *11*, 1330−1339.
(5) Mecozzi, S.; Rebek, J. *Chem.-Eur. J.* **1998**, *4*, 1016−1022.
(6) Bergmann, M.; Fruton, J. S. *J. Biol. Chem.* **1937**, *117*, 189−202.
(7) Fersht, A. *Structure and Mechanism in Protein Science: A Guide to Enzyme Catalysis and Protein Folding*; W. H. Freeman: New York, 1999.
(8) Corma, A.; Iglesias, M.; del Pino, C.; Sanchez, F. *J. Chem. Soc., Chem. Commun.* **1991**, 1253−1255.
(9) Corma, A.; Iglesias, M.; del Pino, C.; Sanchez, F. *J. Organomet. Chem.* **1992**, *431*, 233−246.
(10) Brunet, E. *Chirality* **2002**, *14*, 135−143.
(11) Johnson, B. F. G.; Raynor, S. A.; Shepard, D. S.; Mashmeyer, T.; Thomas, J. M.; Sankar, G.; Bromley, S.; Oldroyd, R.; Gladden, L.; Mantle, M. D. *Chem. Commun.* **1999**, 1167−1168.
(12) Raja, R.; Thomas, J. M.; Jones, M. D.; Johnson, B. F. G.; Vaughan, D. E. W. *J. Am. Chem. Soc.* **2003**, *125*, 14982−14983.
(13) Hultman, H. M.; de Lang, M.; Arends, I. W. C. E.; Hanefeld, U.; Sheldon, R. A.; Maschmeyer, T. *J. Catal.* **2003**, *217*, 275−283.
(14) Jones, M. D.; Raja, R.; Thomas, J. M.; Johnson, B. F. G.; Lewis, D. W.; Rouzaud, J.; Harris, K. D. M. *Angew. Chem., Int. Ed.* **2003**, *42*, 4326−4331.
(15) Sivaguru, J.; Natarajan, A.; Kaanumalle, L. S.; Shailaja, J.; Uppili, S.; Joy, A.; Ramamurthy, V. *Acc. Chem. Res.* **2003**, *36*, 509−521.
(16) Scarso, A.; Shivanyuk, A.; Hayashida, O.; Rebek, J. *J. Am. Chem. Soc.* **2003**, *125*, 6239−6243.
(17) Fiedler, D.; Leung, D. H.; Bergman, R. G.; Raymond, K. N. *J. Am. Chem. Soc.* **2004**, *126*, 3674−3675.
(18) Leung, D. H.; Fiedler, D.; Bergman, R. G.; Raymond, K. N. *Angew. Chem., Int. Ed.* **2004**, *43*, 963−966.
(19) Hart, B. R.; Rush, D. J.; Shea, K. J. *J. Am. Chem. Soc.* **2000**, *122*, 460−465.
(20) Shivanyuk, A.; Scarso, A.; Rebek, J. *Chem. Commun.* **2003**, 1230−1231.

has been previously studied in clathrates and three-dimensional zeolitic pores using ^{2}H NMR spectroscopy.[21,22] Most of these molecules contain a significant amount of molecular motion, albeit less than an isotropic liquid.[23] The relatively rare exception to this, in which the occluded molecule is rigid as in a static situation, has been observed when there are multiple specific interactions, such as via hydrogen bonding, of the occluded molecule with the surrounding framework.[24,25]

Several previous studies of species tethered to a pre-existing two-dimensional silica surface have utilized NMR spectroscopy for measuring the conformational mobility of long-chain aliphatic molecules. In studies on various surface-grafted branched alkoxysilanes,[26,27] as well as long-chain *n*-alkyl silanes,[28−32] several mobility trends have emerged. Carbons in close proximity to the silica surface demonstrate more rigidity and confinement relative to carbons further away from the silica surface,[28] and shorter alkyl chains are more disordered than longer ones.[29] Yet the degree of molecular motion of the bound end in these systems is still relatively high in comparison to a static situation at temperatures above 200 K.[26,29,33]

Our goal is to study the steric confinement of isolated molecules that are tethered to the interior surface of bulk microporous and mesoporous amorphous silicate material networks. Examples of the synthesis of these bulk materials are shown in Scheme 1 (microporous) and Scheme 2 (mesoporous). Our study, in which the tethered species is located within a three-dimensional network, is different from previous studies of molecular motion of tethered species in porous amorphous silicates, which have relied either upon tethering a molecule onto a preexisting two-dimensional surface as illustrated in Scheme 3[26,28,29,34] or upon synthesis of bulk organosilane homopolymers.[27,35] The change in pore size that results from grafting a small molecule onto a surface is small when compared to the pore diameter of preexisting silica supports (60 Å for Selecto 60 and macroporous for Aeroperl 300). For this reason, small molecules postsynthetically tethered to a silica support exist on a two-dimensional surface rather than in any type of three-dimensional confinement.

The fundamental difference of the concurrent bulk synthesis is that it allows the formation of a silicate cage around the occluded molecule, so as to make a locally "tight fit" between it and the amorphous material network during the process of silica condensation. The local "tightness of fit" surrounding the occluded molecule is driven by the requirement for covalent

Scheme 1. Immobilization of **1** in Three-Dimensional Microporous Silicate Network

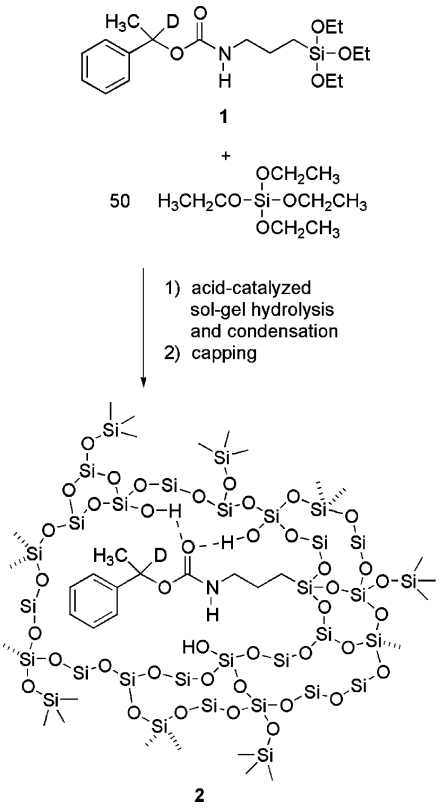

contact between the molecule and the network at the point of tethering, as well as additional specific interactions with the surface, which necessitate silica nucleation in close proximity (distances less than 3.5 Å) to the occluded molecule. The mesoporous silica synthesis used here has been carefully designed to synthesize hierarchical porosity in which a microporous silicate cage is formed around the tethered molecule, while synthesizing mesoporosity in the remainder of the network. If the mesoporous synthesis has been successfully accomplished, the degree of confinement in this material will be similar to bulk microporous material, which contains no mesoporosity.[36]

A critical question that we wish to address is the difference in restricting molecular motion, or equivalently increasing degree of confinement, when using a two-dimensional versus three-dimensional surface for tethering. A second question is whether it is possible to achieve the same degree of steric confinement by synthesizing a bulk mesoporous as compared to a bulk microporous silica network. Here, we investigate molecular motion around the chiral carbon of immobilized molecule **1** using solid-state ^{2}H NMR spectroscopy. The rotational mobility about the C−O axis of molecule **1** involving the chiral carbon is targeted because the end group dynamics are considered to be a good probe for the geometrical confinement of the immediate surroundings of the immobilized carbamate, and ^{2}H NMR spectroscopy is well suited for this purpose. For enabling this study, we have labeled the chiral carbon with deuterium. The nonisotopically enriched isomer of **1** has been used previously for synthesizing bulk, microporous silica via an

(21) Shantz, D. F.; Lobo, R. F. *Top. Catal.* **1999**, *9*, 1−11.
(22) Komori, Y.; Hayashi, S. *Microporous Mesoporous Mater.* **2004**, *68*, 111−118.
(23) Shantz, D. F.; Lobo, R. F. *J. Phys. Chem. B* **1998**, *102*, 2339−2349.
(24) Behrens, P.; van de Goor, G.; Freyhardt, C. C. *Angew. Chem., Int. Ed. Engl.* **1995**, *34*, 2680−2682.
(25) van de Goor, G.; Freyhardt, C. C.; Behrens, P. *Z. Anorg. Allg. Chem.* **1995**, *621*, 311−322.
(26) Kelusky, E. C.; Fyfe, C. A. *J. Am. Chem. Soc.* **1986**, *108*, 1746−1749.
(27) Kang, H.-J.; Blum, F. D. *J. Phys. Chem.* **1991**, *95*, 9391−9396.
(28) Sindorf, D. W.; Maciel, G. E. *J. Am. Chem. Soc.* **1983**, *105*, 1848−1851.
(29) Neumann-Singh, S.; Villanueva-Garibay, J.; Muller, K. *J. Phys. Chem. B* **2004**, *108*, 1906−1917.
(30) Cheng, J.; Fone, M.; Ellsworth, M. W. *Solid State Nucl. Magn. Reson.* **1996**, *7*, 135−140.
(31) Pursch, M.; Brindle, R.; Ellwanger, A.; Sander, L. C.; Bell, C. M.; Handel, H.; Albert, K. *Solid State Nucl. Magn. Reson.* **1997**, *9*, 191−201.
(32) Bayer, E.; Paulus, A.; Peters, B.; Laupp, G.; Reiners, J.; Albert, K. *J. Chromatogr.* **1986**, *364*, 25−37.
(33) Zeigler, R. C.; Maciel, G. E. *J. Am. Chem. Soc.* **1991**, *113*, 6349−6358.
(34) Qiao, Y.; Schonhoff, M.; Findenegg, G. H. *Langmuir* **2003**, *19*, 6160−6167.
(35) Blum, F. D.; Meesiri, W.; Kang, H.-J.; Gambogi, J. E. *J. Adhes. Sci. Technol.* **1991**, *5*, 479−496.
(36) Ini, S.; Defreese, J. L.; Parra-Vasquez, N.; Katz, A. *Mater. Res. Soc. Symp. Proc.* **2002**, *723*, 2.3.1−2.3.7.

Scheme 2. Immobilization of **1** in Three-Dimensional Mesoporous Silicate Network

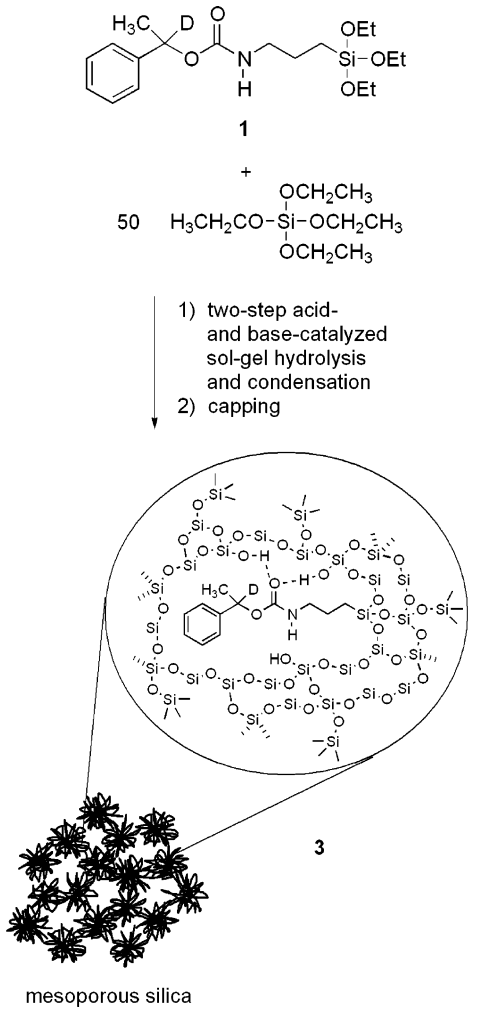

Scheme 3. Immobilization of **1** in Two-Dimensional Mesoporous Silicate Network

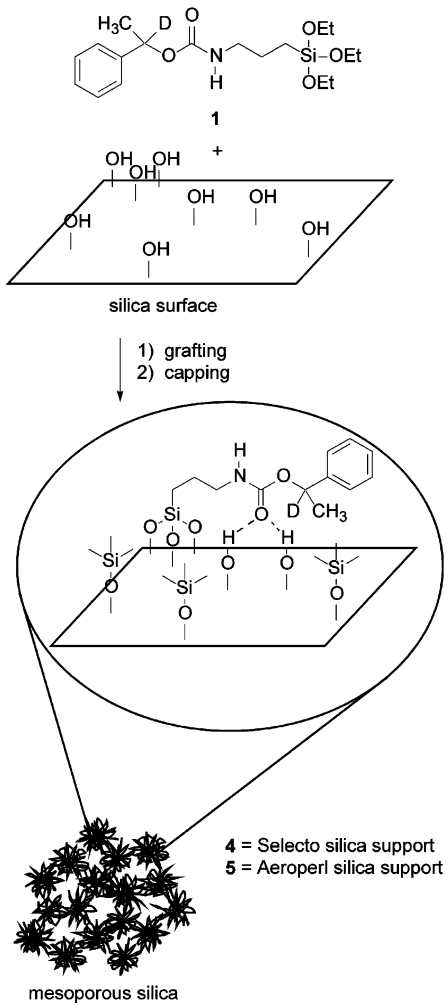

imprinting process, and the resulting imprinted material has recently demonstrated shape-selective adsorption into the imprinted binding pockets.[37]

Experimental Section

Synthesis of 3-Triethoxysilylpropyl-carbamic Acid 1-Phenyl-1-deutero-ethyl Ester (1). The molecule was prepared from the parent alcohol by standard coupling procedures.[38] To a solution of 1,1′-carbonyldiimidazole (6.71 g, 41.4 mmol) and a catalytic amount of sodium ethoxide in anhydrous THF (60 mL) was added neat 1-phenylethan-1-d_1-ol (5.0 g, 40.6 mmol). The solution was stirred at room temperature for 12 h prior to the addition of 3-(aminopropyl)-triethoxysilane (10.0 mL, 42.7 mmol). The solution was then stirred for 3 h at room temperature. Following solvent removal, excess imidazole was precipitated with hexane and removed by filtration. The crude product was purified by column chromatography (Silica Gel 60, 2/1 v/v hexane/ethyl acetate) to yield a clear oil (11.53 g, yield 77%). ^{1}H NMR 400 MHz ($CDCl_3$) δ (ppm): 0.618−0.659 (2H, m, CH_2-$CH_2CH_2Si(OCH_2CH_3)_3$); 1.241 (9H, t, J = 7.0 Hz, $Si(OCH_2CH_3)_3$); 1.534 (3H, s, $PhCD(CH_3)O$); 1.595−1.670 (2H, m, $CH_2CH_2CH_2Si$-$(OCH_2CH_3)_3$); 3.114−3.207 (2H, m, $CH_2CH_2CH_2Si(OCH_2CH_3)_3$); 3.832 (6H, q, J = 7.0 Hz, $Si(OCH_2CH_3)_3$); 5.145 (1H, bs, N*H*); 7.235−7.565 (5H, m, Ar−*H*). ^{13}C{^{1}H} NMR 400 MHz ($CDCl_3$) δ (ppm): 7.6 (CH_2-CH_2CH_2Si); 18.3 ($Si(OCH_2CH_3)_3$); 22.4 ($PhCD(CH_3)O$); 23.3 (CH_2CH_2-CH_2Si); 43.4 ($CH_2CH_2CH_2Si$); 58.4 ($Si(OCH_2CH_3)_3$); 126.0 (Ar−*C*); 127.6 (Ar−*C*); 128.4 (Ar−*C*); 142.3 (C_q); 156.0 (*C*═O). Mass spectrum (FAB$^+$): *m*/*z* 371.2121 ($C_{18}H_{31}DNO_5Si$, 371.2112).

Bulk Microporous Materials Synthesis. The bulk microporous material was synthesized according to published procedures.[37,39]

Bulk Mesoporous Materials Synthesis. The mesoporous material was synthesized by dissolving 1.80 mmol of **1** (0.668 g) and 89.6 mmol of TEOS (20 mL) in 63 mL of absolute ethanol. The solution was brought to reflux, and the following aliquots were added at 1 h intervals: 0.5 mL of pH 2.0 *p*-toluenesulfonic acid, 0.5 mL of pH 2.0 *p*-toluenesulfonic acid, 3.9 mL of water, and 3.9 mL of water. The solution was refluxed for 1 h after the last water addition. After 10 min of cooling, the solution was added to 4.4 mL of aqueous ammonium hydroxide (pH 11.7) under vigorous stirring. After the material formed an optically transparent gel, it was aged for 24 h at room temperature and then dried in an oven at 40 °C for at least 10 days. The silica monoliths were ground to <10 μm particles and Soxhlet extracted for 24 h in anhydrous acetonitrile refluxing over calcium hydride.

Surface-Grafted Mesoporous Materials Synthesis. The surface-grafted materials were prepared by dissolving 0.1 mmol of **1** in 20 mL of glacial acetic acid. To the solution was added 2 g of Selecto 60 or Aeroperl 300 silica. The mixtures were stirred at 75 °C overnight. The silica was then filtered and Soxhlet extracted in anhydrous benzene refluxing over calcium hydride.

Materials Capping and Deprotection Procedures. The framework silanol groups on each of the materials were capped with trimethylsilyl

(37) Defreese, J. L.; Katz, A. *Microporous Mesoporous Mater.* **2006**, *89*, 25−32.
(38) Staab, H. A. *Angew. Chem., Int. Ed. Engl.* **1962**, *1*, 351−367.
(39) Defreese, J. L.; Katz, A. *Chem. Mater.* **2005**, *17*, 6503−6506.

(TMS) groups according to published procedures.[37,39,40] To confirm site-isolation, carbamates in surface-grafted material **4** were subjected to deprotection via published procedures,[37] which synthesized primary amines for use in catalysis experiments via cleavage of the carbamate bond in the immobilized **1**.

FT-IR Sample Preparation. Prior to sample preparation, the potassium bromide was dried at 300 °C under vacuum for at least 12 h. The silica materials were dried at 120 °C under vacuum for at least 12 h. Sample pellets were prepared using a hydraulic press, with 3−10 mg of silica material in approximately 200 mg of potassium bromide. The FT-IR spectra were recorded on a N_2-purged instrument, with each spectrum the average of 128 interferograms and covering a spectral range from 4000 to 400 cm^{-1}. For each of the materials, both the protected (**1** intact) and the deprotected materials were examined. Because of the low abundance of **1** within the silica material, each deprotected material was subtracted from the protected material to selectively observe the characteristic bands due to immobilized carbamate.

Results and Discussion

Materials Synthesis and Characterization. Our materials synthesis procedures are carefully designed to ensure isolation of the immobilized carbamate molecules. Previous studies of molecular motions of surface-tethered complexes have shown that high surface coverages influence the mobility of alkyl chains on a silica surface,[26−30,33,34,41] because the resulting mobility is modified by a combination of intermolecular interactions between tethered species and steric effects of the surface.[27,31,33,41,42] We are interested in isolating immobilized **1** to minimize the effect of intermolecular interactions between adjacent tethered molecules and ensure that we are investigating the level of confinement that arises due to the rigid silica network itself. In the surface-functionalized materials, isolation of immobilized **1** is facilitated primarily through statistical isolation by grafting to a preexisting silica surface at low surface coverage. Although we cannot completely rule out some degree of imprint−imprint intermolecular contact in the materials, we have no evidence to indicate the presence of imprint−imprint interactions in our materials. Catalysis data on materials consisting of primary amines synthesized via deprotection of materials used in this study demonstrate that all of our materials lack the type of intersite aggregation observed in conventional amine-on-silica materials (vide infra).

In the bulk amorphous materials, **1** is immobilized concurrently with silica synthesis, allowing the possibility of three-dimensional steric confinement via formation of a silicate cage around the occluded molecule. This process may be driven by noncovalent interactions between **1** and the silica precursors in addition to the covalent nucleation site at the terminus of the aminopropyl tether.[43] Site isolation is ensured in the microporous material via both statistical isolation of **1** (2 mol % relative to silica network precursors), as well as by conducting the synthesis under acid-catalyzed conditions that promote a similar hydrolysis and condensation rate for the organosilane and the silica network precursors to minimize self-condensation and potential aggregation of condensed organosilane **1**.[44,45]

The mesoporous materials synthesis was carefully designed to create a material with hierarchical porosity, possessing microporous active sites to accomplish confinement of **1** and a mesoporous framework for facilitating mass transport. The synthetic strategy is based on a two-step acid−base sol−gel hydrolysis[44−46] that avoids the use of surfactants[47] or block copolymers,[48] which could potentially cause local phase separation and aggregation of tethered species within hydrophobic domains of a micellar structure. The initial acid-catalyzed step synthesizes small oligomers of silica that condense around isolated species of hydrolyzed **1**,[44,45] with low water content contributing to maintenance of conditions favoring random copolymerization of the silica precursor and **1**.[49] This acid step that synthesizes a silicate shell around immobilized **1** is followed by a base-catalyzed hydrolysis that synthesizes bulk mesoporosity during condensation. The resulting glass is optically clear with no visible phase separation, as opaqueness can be indicative of aggregation processes within the bulk solid.[50] The material also displays the desired bimodal pore size distribution, containing both active site microporosity and bulk network mesoporosity.[36,51] A base-catalyzed probe reaction consisting of the Knoevenagel condensation of isophthalaldehyde and malononitrile[52] was used to confirm the improved mass transport characteristics of the bulk mesoporous material over its microporous analogue. The mesoporous material possessed an observed turnover frequency 30-fold higher than that measured for the analogous microporous material. The lack of mass transport limitations in the mesoporous materials has enabled studies of outer-sphere acidity effects on catalysis with comparisons between bulk materials and conventional surface-functionalized materials.[40]

In bulk amorphous silicas utilizing an occluded carbamate similar to **1**, site isolation was demonstrated via chemisorption of a pyrene fluorescence probe to tethered primary amines resulting from carbamate deprotection. These sites showed primarily monomer pyrene emission signature in comparison to majority excimer in conventional aminopropylsilane-modified silica.[51] We have further shown that the degree of site isolation as ascertained by pyrene fluorescence correlates to shape-selectivity of a sequential base-catalyzed probe reaction that we have used previously for characterizing imprinted materials.[40,52] This was performed by showing that reaction of isophthalaldehyde and malononitrile produces two products: a monosubstituted product and a disubstituted product, in which both aldehydes have reacted. Conducting the reaction using a site-isolated catalyst inhibits the immediate formation of disubstituted relative to monosubstituted product, whereas a clustered amine catalyst produces both disubstituted and monosubstituted products immediately.[36] Thus, initial reaction selectivity is a sensitive indicator of the degree of local aggregation of the catalytic amine active sites, and, for this reason, catalysis of this reaction was used in the current study as a probe to verify site isolation of

(40) (a) Bass, J. D.; Anderson, S. L.; Katz, A. *Angew. Chem., Int. Ed.* **2003**, *42*, 5219−5222. (b) Bass, J. D.; Solovyov, A.; Pascall, A. J.; Katz, A. *J. Am. Chem. Soc.* **2006**, *128*, 3737−3747.
(41) Zeigler, R. C.; Maciel, G. E. *J. Phys. Chem.* **1991**, *95*, 7345−7353.
(42) Pursch, M.; Sander, L. C.; Albert, K. *Anal. Chem.* **1996**, *68*, 4107−4113.
(43) Katz, A. The Synthesis and Characterization of Molecularly Imprinted Materials. Ph.D. Thesis, California Institute of Technology, Pasadena, CA, 1999.
(44) Brinker, C. J.; Keefer, K. D.; Schaefer, D. W.; Ashley, C. S. *J. Non-Cryst. Solids* **1982**, *48*, 47−64.
(45) Brinker, C. J.; Keefer, K. D.; Schaefer, D. W.; Assink, R. A.; Kay, B. D.; Ashley, C. S. *J. Non-Cryst. Solids* **1984**, *63*, 45−59.
(46) Cao, G. Z.; Tian, H. *J. Sol.-Gel Sci. Technol.* **1998**, *13*, 305−309.
(47) Dai, S. *Chem.-Eur. J.* **2001**, *7*, 763−768.
(48) Coutinho, D.; Acevedo, A. O.; Dieckmann, G. R.; Balkus, K. J. *Microporous Mesoporous Mater.* **2002**, *54*, 249−255.
(49) Sugahara, Y.; Inoue, T.; Kuroda, K. *J. Mater. Chem.* **1997**, *7*, 53−59.
(50) Katz, A.; Davis, M. E. *Macromolecules* **1999**, *32*, 4113−4121.
(51) Bass, J. D.; Katz, A. *Chem. Mater.* **2003**, *15*, 2757−2763.
(52) Katz, A.; Davis, M. E. *Nature* **2000**, *403*, 286−289.

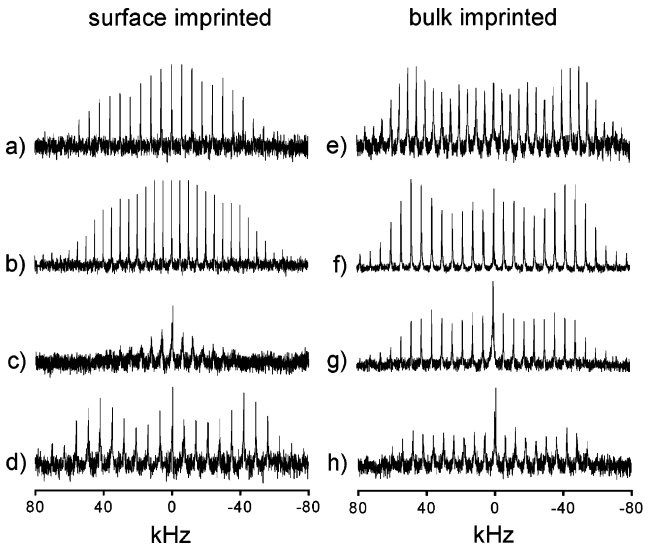

Figure 1. ^{2}H MAS spectra of (a) surface material **5** (Aeroperl) at room temperature, (b) surface material **4** (Selecto) at room temperature, (c) surface material **4** (Selecto) at 413 K, (d) surface material **4** (Selecto) at 213 K, (e) bulk microporous material **2** at room temperature, (f) bulk mesoporous material **3** at room temperature, (g) bulk microporous material **2** at 413 K, and (h) bulk mesoporous material **3** at 413 K.

the materials. This required that the tethered **1** illustrated in Scheme 1−3 be deprotected with iodotrimethylsilane to liberate primary amines for use in catalysis (see Supporting Information for details). With confirmation of the framework porosity and site isolation of each of the materials, we then investigated the confinement of **1** in the bulk amorphous materials.

NMR Spectroscopy Results. To analyze the degree of confinement and compare between different materials, we utilized solid-state ^{2}H MAS NMR spectroscopy to assess the molecular motion of **1** immobilized in each of the three types of materials: bulk microporous (**2**), bulk mesoporous (**3**), and surface-functionalized (**4** and **5**). The degree of molecular mobility of immobilized **1**, particularly around the C−O bond axis involving the chiral carbon, correlates inversely with degree of confinement. Because of the relatively high dilution of immobilized **1** in silica in each of the materials, the ^{2}H MAS NMR technique was chosen rather than the corresponding wide-line static NMR spectroscopic methods to circumvent limitation due to signal sensitivity.[23,53] ^{2}H MAS NMR spectroscopy is generally useful for investigating molecular motion with correlation times ranging between 10^{-3} s and 10^{-8} s.[53,54]

As shown in Figure 1a and 1b, there is rapid molecular motion (time scale faster than 10^{-7} s) in the surface-functionalized materials **4** and **5** at room temperature. The shape of the powder pattern can be fit to a simple two-site hopping mode of motion.[54] This mobility is consistent with the results in the previously described examples for the rotational mobility of long chain aliphatic compounds grafted to the surface of silica.[26,28,29,31,34] However, unlike the previous systems, which still display significant molecular motion even when cooled to 200 K,[26,29,33] the surface-functionalized material **4** shows a significant "freezing out" of the motion at 213 K (Figure 1d), with the quadrupole powder pattern exhibiting recovery of the Pake doublet.[53,54] The correlation time τ_c in Figure 1d is larger than 10^{-2} s, and is consistent with either a slower jumping motion or a static C−D bond with librational motion, although it is not possible to tell the difference between the two. This restriction of molecular motion at lower temperature suggests that there is a larger activation energy for motion involving the C−D bond in this system than for tethered alkyl chains on silica surfaces.[26,29,33] This activation energy may be increased due to interactions between the carbamate carbonyl and the silica surface, which may help organize the tethered molecule close to the silica surface in its immobilized form (vida infra), resulting in greater rigidity as observed in other systems, where long aliphatic chains display less motion for carbons close to the silica surface and increasing motion for those further away.[26,28,33,41] The motion of tethered molecule **1** is identical on both silica surfaces investigated, Selecto and Aeroperl, with faster hopping motion of the C−D bond at room temperature and reduced hopping rate at 213 K. The rapid molecular motion indicates that **1** is not sterically confined in the surface-grafted materials at room temperature.

It should be easiest to achieve steric confinement of tethered **1** in the bulk microporous silica framework (**2**), because the size of the micropores is commensurate with small molecule dimensions.[52] However, even for microporous material **2**, achieving confinement looks less clear-cut when compared to previous studies of nontethered molecules in microporous systems. In systems of cyclophosphazene inclusion compounds, rapid rotational motion of benzene[55] as well as *p*- and *o*-xylene[56] is observed even at low temperatures of 150 K. In a study of benzyltrimethylammonium cation structure directing agents (SDAs) occluded in an as-made microporous zeolite, it was shown that, although the SDAs experienced a reduced number of possible configurations, they still experienced significant motion, particularly in rapid rotation of the trimethylammonium segment.[57] The implication of these and similar studies is that the mere presence of a micropore is insufficient for restricting molecular motions of small molecules, particularly in untethered form.

The effect of confinement on rotional mobility of tethered **1** by the microporous framework is shown in Figure 1e. The time scale for the hopping motion τ_c is estimated to be greater than 10^{-2} s using the same quadrupole interaction parameters as used in the simulation of the surface-grafted materials (Table 1). This value is comparable to values observed in the surface-grafted materials at 213 K. However, it is significantly larger than the τ_c value observed in the surface-grafted materials at room temperature, indicating that immobilized **1** is significantly more confined in the bulk microporous material. Achieving the "tightness of fit" of steric confinement in the bulk mesoporous network of **3** is synthetically more challenging relative to the microporous **2**. Because of the bulk mesoporosity of the framework, it could be possible for **1** to be grafted to the interior mesoporous surface of **3**, not unlike the postsynthetically grafted **1** in materials **4** and **5**. This is because immobilizing **1** on a preexisting silica surface produces anchored molecules that sample the entire interior porosity, most of which is mesoporous

(53) Hologne, M.; Hirschinger, J. *Solid State Nucl. Magn. Reson.* **2004**, *26*, 1−10.
(54) Jelinski, L. W. High-Resolution NMR Spectroscopy of Synthetic Polymers in Bulk. *Methods in Stereochemical Analysis*; VCH: Deerfield Beach, FL; Vol. 7, pp 335−364.
(55) Meirovitch, E.; Belsky, I.; Vega, S. *J. Phys. Chem.* **1984**, *88*, 1522−1526.
(56) Meirovitch, E.; Belsky, I. *J. Phys. Chem.* **1984**, *88*, 4308−4315.
(57) Shantz, D. F.; Fild, C.; Koller, H.; Lobo, R. F. *J. Phys. Chem. B* **1999**, *103*, 10858−10865.

Table 1. Estimated Correlation Time (τ_c) by Using a Two-Site Hopping Model

material scaffold	correlation time (s)[a]
2 (bulk microporous) at room temperature	$>10^{-2}$
3 (bulk mesoporous) at room temperature	$>10^{-2}$
4 (surface Selecto 60) at room temperature	$<10^{-7}$
4 (surface Selecto 60) at 213 K	$>10^{-2}$
2 (bulk microporous) at 413 K	$\sim10^{-3}-10^{-4}$
3 (bulk mesoporous) at 413 K	$\sim10^{-3}-10^{-4}$

[a] A single correlation time, quadrupole coupling constant QCC = ~155 kHz, and asymmetry parameter $\eta_Q = 0$ were used for simulating the ^{2}H MAS spectra.

for **3**.[36,51] We carefully designed the mesoporous materials synthesis for **3** to synthesize a microporous cage around each immobilized **1** while synthesizing mesoporosity in the remainder of the material framework. As shown in Figure 1f, the NMR spectroscopic data support the existence of silicate cages that provide steric confinement for immobilized **1**. At room temperature, **1** occluded within the bulk mesoporous material **3** displays similar limited molecular mobility ($\tau_c > 10^{-2}$ s) as observed in the microporous material **2**, including the same characteristic powder pattern and quadrupole parameters. Because there is essentially no observed difference in molecular mobility between the microporous and mesoporous frameworks, the mesoporous materials synthesis procedure discovered has indeed been successful in creating sterically confining micropores within the bulk mesoporous framework while retaining hierarchical porosity and associated advantages of improved accessibility and mass transport (vide supra).

We have also examined the surface-functionalized and bulk materials at a higher temperature to investigate how effectively steric confinement of **1** is preserved in the presence of additional thermal energy. We chose a temperature of 413 K, because it is a temperature at which we have carefully verified the stability of tethered **1** in air via thermogravimetric analysis. The surface-functionalized material **4** at 413 K exhibits significant narrowing of the entire powder pattern (Figure 1c) relative to the room-temperature spectrum (Figure 1b). This is indicative of additional degrees of freedom via an increasing combination of motional modes so that the anisotropic character of the quadrupole coupling is being gradually averaged out. Additionally, when compared to the room-temperature spectrum (Figure 2a), the line width of the individual spinning sidebands is broadened at 413 K (Figure 2b), which is consistent with a higher amount of librational motion that is nonspecific to the C−D bond at elevated temperature and the time scale of which begins to interfere with the magic angle spinning rate. Returning the surface-imprinted material **4** to room temperature (Figure 2c) results in a return of the narrow line width, a reversibility that confirms lack of sample degradation at elevated temperature.

Microporous material **2** (Figure 1g) and mesoporous material **3** (Figure 1h) show only slight narrowing of the powder pattern at 413 K and retain the characteristic Pake doublet quadrupole pattern, with only minor changes in the hopping rate relative to the surface-grafted material at room temperature (Table 1). This confirms that the steric confinement of the bulk mesoporous material is the same as the bulk microporous material even at elevated temperatures. As observed for surface-grafted material **4**, materials **2** (Figure 2f) and **3** (Figure 2e) experience some broadening of individual spinning sideband line widths at higher temperature as compared to room temperature (Figure 2d). The origin of this line broadening is mainly caused by the slightly increased hopping rate around the same C−O bond axis, as manifested in the change from $\tau_c > 10^{-2}$ s to $\tau_c \approx 10^{-3}$ s-10^{-4} s. Rotational motion with this new correlation time subsequently interferes with the magic angle spinning rate to cause the observed broadening. The distortion of the overall powder pattern from room-temperature spectra is not well-understood, and it may result from a number of potential causes such as an increased contribution of jumping angle distribution, libration, or wobble motions.[53,60,61] In addition, a sharp component is observed for all of the materials studied and is unrelated to C−D bond dynamics. Such a phenomenon may be due to trapped moisture and should not be interpreted as the emergence of a sharp component due to motional averaging.

As the NMR spectroscopy results above demonstrate, immobilized **1** is sterically confined within the bulk materials even at temperatures as high as 413 K, and this is in stark contrast to its state in the surface-grafted materials at room temperature. This requires silica nucleation near immobilized **1** during pore formation in **2** and **3**. The one known point of nucleation is at the aminopropyl tether, where **1** covalently condenses to the silica network precursors. However, to create a well-formed pore capable of true three-dimensional steric confinement, additional interactions between the silica surface and immobilized **1** may facilitate confinement during the process of materials synthesis via sol−gel hydrolysis and condensation. To investigate the potential interactions of the carbonyl group of the carbamate **1** with the silica of the pore wall, we examined each of the materials by solid-state FT-IR spectroscopy.

FT-IR Spectroscopy Results. FT-IR spectroscopy is a sensitive tool for exploring the effect of hydrogen bonding and polarization of the dielectric environment surrounding the carbonyl functionality of carbamate **1**. Carbonyls not only show a very strong characteristic stretching band in the IR spectrum, but this band also shifts from higher to lower wavenumbers when going from noninteracting to either hydrogen-bonded or higher dielectric constant environments.[62,63] Hydrogen bonding between residual silanols and amide carbonyls has been studied previously and shown to shift the carbonyl stretching band to lower wavenumbers by 12−25 cm^{-1} relative to the neat amide,[64,65] and a similar lowering of the carbonyl band frequency has also been observed due to dielectric effects upon dissolution of neat amide in a solvent such as DMSO.[63,66]

Table 2 shows the results of FT-IR measurements at room temperature. All of the silica materials clearly display a shift

(58) Laupretre, F.; Monnerie, L.; Virlet, J. *Macromolecules* **1984**, *17*, 1397−1405.
(59) Pivcova, H.; Saudek, V.; Schmidt, P.; Hlavata, D.; Plestil, J.; Laupretre, F. *Polymer* **1987**, *28*, 991−997.
(60) Goddard, Y. A.; Vold, R. L.; Hoatson, G. L. *Macromolecules* **2003**, *36*, 1162−1169.
(61) Malyarenko, D. L.; Vold, R. L.; Hoatson, G. L. *Macromolecules* **2001**, *34*, 7911−7915.
(62) Pimentel, G. C.; McClellan, A. L. *The Hydrogen Bond*; W. H. Freeman: San Francisco, CA, 1960.
(63) (a) Torii, H.; Tasumi, M. *J. Raman Spectrosc.* **1998**, *29*, 537−546. (b) Kubelka, J.; Keiderling, T. A. *J. Phys. Chem. A* **2001**, *105*, 10922−10928.
(64) Ogoshi, T.; Chujo, Y. *Bull. Chem. Soc. Jpn.* **2003**, *76*, 1865−1871.
(65) Saegusa, T. *Pure Appl. Chem.* **1995**, *67*, 1965−1970.
(66) Eaton, G.; Symons, M. C. R.; Rastogi, P. P. *J. Chem. Soc., Faraday Trans.* **1989**, *85*, 3257−3271.

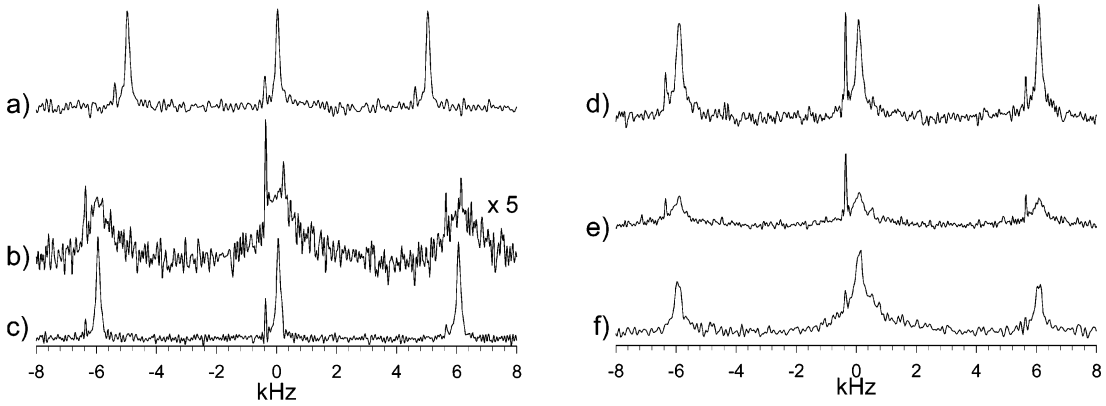

Figure 2. ^{2}H MAS NMR spectra displayed for the center and the first spinning sidebands of: (a) surface-grafted material **4** at room temperature, (b) surface-grafted material **4** at 413 K, (c) surface-grafted material **4** after a return to room temperature, (d) mesoporous material **3** at room temperature, (e) mesoporous material **3** at 413 K, and (f) microporous material **2** at 413 K. The spinning rate is 6 kHz in all spectra, except (a) where it is 5 kHz.

Table 2. FT-IR Carbonyl Stretching and Isolated Silanol Frequencies for Silica Materials

material scaffold	C=O stretch (cm^{-1})[b]	isolated silanol band (cm^{-1})[c]	surface coverages (mmol/g)
noninteracting **1**[a]	1726 ± 2	n/a	n/a
neat **1**	1711 ± 10	n/a	n/a
2 (bulk microporous)	1699 ± 2	3739 ± 2	0.28
3 (bulk mesoporous)	1701 ± 2	3739 ± 2	0.26
4 (surface Selecto 60)	1703 ± 2	3739 ± 2	0.21
5 (surface Aeroperl 300)	1703 ± 2	3739 ± 2	0.098

[a] 0.01 M of **1** in CCl_4. [b] From subtraction spectrum of protected and deprotected materials. [c] From spectrum of materials deprotected with trimethylsilyliodide.

of approximately 20 cm^{-1} in the carbonyl band as compared to the noninteracting **1** at 0.01 M in CCl_4, and a measurable shift with respect to the carbonyl band for neat carbamate **1**. However, there is no discernible difference in the position of the carbonyl band for immobilized **1** between surface-grafted and bulk materials. Because trimethylsilyl capping in materials **2**−**4** still leaves behind residual uncapped silanols that remain in the framework of each of the materials, particularly for silanols that may be sterically hindered,[67] the observed shifts may be due to either specific hydrogen bonds between the carbonyl and silanols or the presence of a more polarized dielectric environment due to the nearby presence of the silica surface. Evidence for silanols remaining despite trimethylsilyl capping is provided by a relatively sharp isolated silanol infrared band centered near 3740 cm^{-1} in all materials investigated.

The similar shift of the carbonyl stretching band in the FT-IR spectrum of each of the materials indicates that the carbonyl groups in both surface- and bulk-immobilized **1** are not within a gas-phase environment and are affected by electrostatic interactions with the silica surface. Because of the flexibility of the aminopropyl tether in immobilized **1**, we postulate that it may be possible for the carbonyl to hydrogen bond with residual silanols, even in the surface-grafted materials, given the conformational flexibility in **1** and as previously described for molecules anchored with propyl tethers on silica.[68] One possibility is a double[69] hydrogen-bonding arrangement, which is illustrated in Schemes 1−3, whereas another possibility involves no hydrogen-bonding interaction and involves instead solvation by the silica surface, which causes polarization of the dielectric environment surrounding the carbonyl.[63,66] The fact that all three classes of materials show the same shift of the carbonyl band indicates an energetic driving force for **1** to nucleate close to the silica surface in the region of the carbonyl. During bulk silica hydrolysis and condensation, this driving force may assist in pore-wall formation, which creates a cage of silica closely around immobilized **1**, thereby sterically confining the molecule to the extent that rotation is significantly limited in both the bulk microporous and the bulk mesoporous materials. These observations of carbonyl interaction with the silica surface even after extensive capping are supported by the catalytic data of Corma and co-workers, who observed significant support effects on active site reactivity even in capped silica materials.[70]

Conclusions

We have investigated and compared the steric confinement of isolated tethered molecules within three types of material networks: two-dimensional silica surface, bulk amorphous microporous silica, and bulk amorphous mesoporous silica. The ^{2}H MAS NMR study unequivocally demonstrates that the bulk materials achieved thorough steric confinement of the immobilized **1**, severely limiting molecular mobility at both room temperature and elevated temperature. This result is remarkable in light of the previously explored systems, which generally displayed significant restrictions of molecular motion only at very low temperatures[26,29] or in the presence of multiple strong hydrogen bonds.[24,25]

These conclusions are supported by FT-IR spectroscopic evidence that demonstrates that the silica surface can interact with the carbonyl functionality of **1**, causing an observable shift of the carbonyl band in the IR spectrum. The fact that the silica surface after TMS-capping can influence the shift of the carbonyl peak in the IR suggests that similar interactions between the carbonyl of the occluded molecule and silica precursors may play an important role in nucleating the formation of a pore wall close to **1** during materials synthesis.

These results comprise the first explicit proof of tethered molecule confinement within bulk amorphous silica. There is

(67) Little, C. J.; Whatley, J. A.; Dale, A. D. *J. Chromatogr.* **1979**, *171*, 435−438.
(68) Caravajal, G. S.; Leyden, D. E.; Quinting, G. R.; Maciel, G. E. *Anal. Chem.* **1988**, *60*, 1776−1786.
(69) Pihko, P. M. *Angew. Chem., Int. Ed.* **2004**, *43*, 2062−2064.
(70) Baleizao, C.; Gigante, B.; Garcia, H.; Corma, A. *J. Catal.* **2003**, *216*, 199−207.

broad potential for imparting significant steric confinement on occluded molecular guests using bulk amorphous silica as a synthetic host, which is difficult to accomplish via other methods of host−guest encapsulation.[5,20] The difficult-to-achieve confinement of isolated functional groups demonstrated here has particular implications in fundamental studies and technological applications exploiting confinement such as in selective heterogeneous catalysis and adsorption,[71] as well as photoluminescence.[72,73]

Acknowledgment. We thank Dr. Maggy Hologne and Dr. Jerome Hirschinger at CNRS, Universite Louis Pasteur, France, and Dr. Sungsool Wi at Virgina Polytechnical Institute and State University for sharing ^{2}H MAS NMR simulation software. We gratefully acknowledge the National Science Foundation (CTS 0407478) for financial support, as well as a graduate research fellowship for J.L.D. S.-J.H. acknowledges the National Science Foundation under Grant Number 9724240 and the MRSEC Program of the National Science Foundation under Award Number DMR-0080065 for supporting the Caltech Solid State NMR facility.

Supporting Information Available: Evidence for site isolation. This material is available free of charge via the Internet at http://pubs.acs.org.

JA0556474

(71) Davis, M. E.; Katz, A.; Ahmad, W. R. *Chem. Mater*. **1996**, *8*, 1820−1839.
(72) Ostafin, A.; Siegel, M.; Wang, Q.; Mizukami, H. *Microporous Mesoporous Mater.* **2003**, *57*, 47−55.
(73) Makarova, O.; Ostafin, A.; Miyoshi, M.; Norris, J. *J. Phys. Chem. B* **1999**, *103*, 9080−9084.